We are IntechOpen,
the world's leading publisher of
Open Access books
Built by scientists, for scientists

4,800
Open access books available

122,000
International authors and editors

135M
Downloads

Our authors are among the

154
Countries delivered to

TOP 1%
most cited scientists

12.2%
Contributors from top 500 universities

BOOK
CITATION
INDEX
CLARIVATE ANALYTICS
INDEXED

WEB OF SCIENCE™

Selection of our books indexed in the Book Citation Index
in Web of Science™ Core Collection (BKCI)

Interested in publishing with us?
Contact book.department@intechopen.com

3D Nonlinear Finite Element Plastic Analysis of Cylindrical Vessels Under In-Plane Moment

B.H. Wu

Additional information is available at the end of the chapter

1. Introduction

Cylindrical vessels with nozzles are common structural components in many industries, such as power engineering, petrochemical, etc. Under the applied pressure and piping loads, a high stress concentration is caused by the geometric discontinuity. The connection region of the vessel and nozzle will become the weakest location of the entire structure. Therefore, it is necessary to have an accurate design method for the structure. The plastic limit design method is one possibility. In design, a gross plastic deformation is prevented by restricting the allowable load relative to the plastic limit load of the vessels. Therefore, the key step in limit design is to determine the plastic limit load of the vessels under different loads.

The plastic limit load estimate for practical engineering materials (with strain hardening and geometrical strengthening) can be determined by the twice-elastic-slope (TES) criterion [1]. Many approaches to determine the plastic limit load have been contributed by a number of authors employing analytical, experimental and finite element methods for components under internal pressure, and nozzle or branch pipe loading. Ellyin[2] [3] reported experimental results for the elastic-plastic behavior and plastic limit loads of five tee-shaped cylinder-cylinder intersections under internal pressure, and in-plane or out-of-the-plane moment. The results indicated that the out-of-plane loading case was the critical one. Schoreder[4] provided experimental limit branch moment loads on 4-in. ANSI B16.9 Tees using different limit load criteria. The results of the study showed that the branch moment capacity for the tee models was greater than the theoretical limit load of the equivalent nominal size straight pipe. Junker[5] performed inelastic finite element analyses to estimate the limit moment for a cylindrical vessel with a nozzle subjected to in-plane and out-of-plane moment loadings. The results indicated that the predicted limit moment levels agree to within 10% with the experimental results and that the finite element

method gives a reasonably accurate determination of limit moments for cylindrical vessels with nozzles under in-plane and out-of-plane moments. Moffat[6] performed an experimental study of branch connections subjected to external moment loadings. Further, in 1991, Moffat et al.[7] provided extensive numerical results for the effective stress factor of branch junctions under internal pressure and external moment loads. An empirical formula was presented using polynomial equations. Rodabaugh[8] [9] contributed a valuable review of limit loads for pipe connections in pressure vessels and piping. In the review, a comprehensive overview of pipe connections was provided. Other studies [10]~[13] carried out important works on plastic limit analysis of cylindrical vessels under external nozzle loadings.

The objective of this paper is to determine the plastic limit moment by both experiment and finite element analysis for cylindrical vessels under in-plane moment loading on the nozzle. Based on these results, a parametric analysis is carried out and an empirical formula is proposed.

2. Experimental study

2.1. Model vessels

Three model vessels with different d/D ratios were designed and fabricated for the experimental study. Every model vessel consisted of a cylinder, nozzle, and flanges for fixing and loading bars. Figure 1 shows a typical configuration, and dimensions for the model vessels are listed in Table 1.
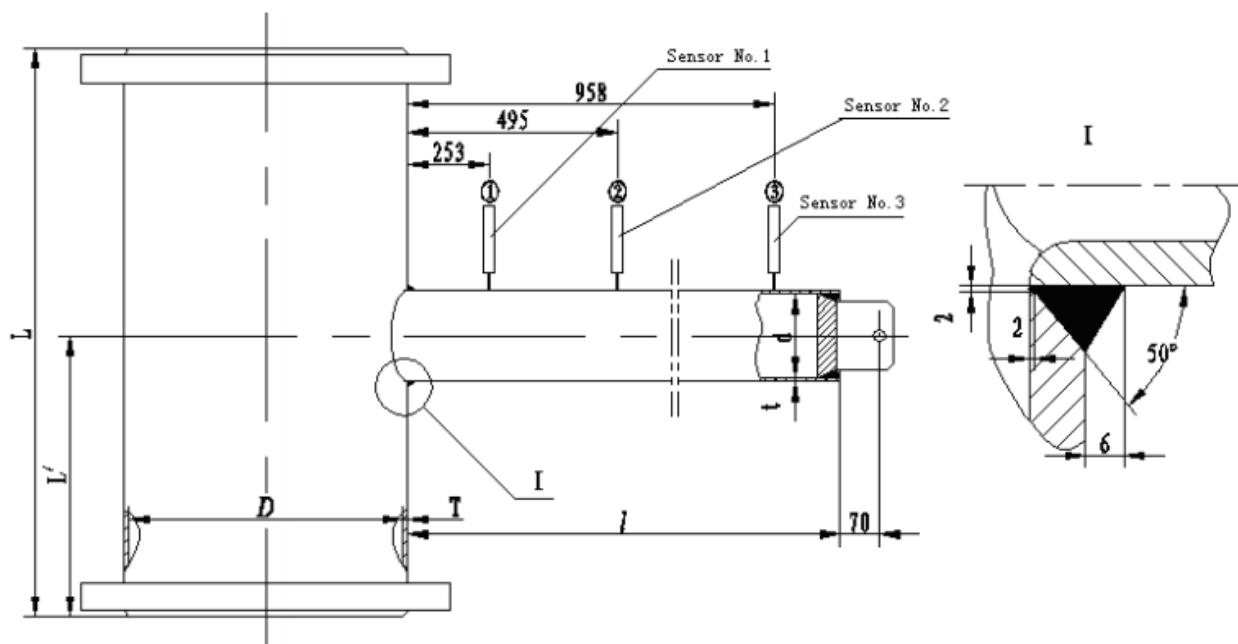

Figure 1. Arrangement of model vessels (mm)

	D(mm)	L(mm)	L' (mm)	T(mm)	d(mm)	l(mm)	t(mm)	d/D	t /T	D / T
L_1	500	1000	500	8	86	1000	3	0.172	0.375	62.5
L_2	500	1000	500	8	123	1000	4	0.246	0.50	62.5
L_3	500	1000	500	8	214	1000	5	0.428	0.625	62.5

Table 1. Dimensions of model vessels

The materials of the cylinder and the nozzle are Q235-A (low carbon steel, similar to A36-77) and 20# (low carbon steel, similar to A106-80 GrA), respectively. Detailed chemical composition and mechanical properties of materials are given in Reference [14]. Figure 2 shows the engineering stress-strain curve of materials for Q235-A and 20# Steel.
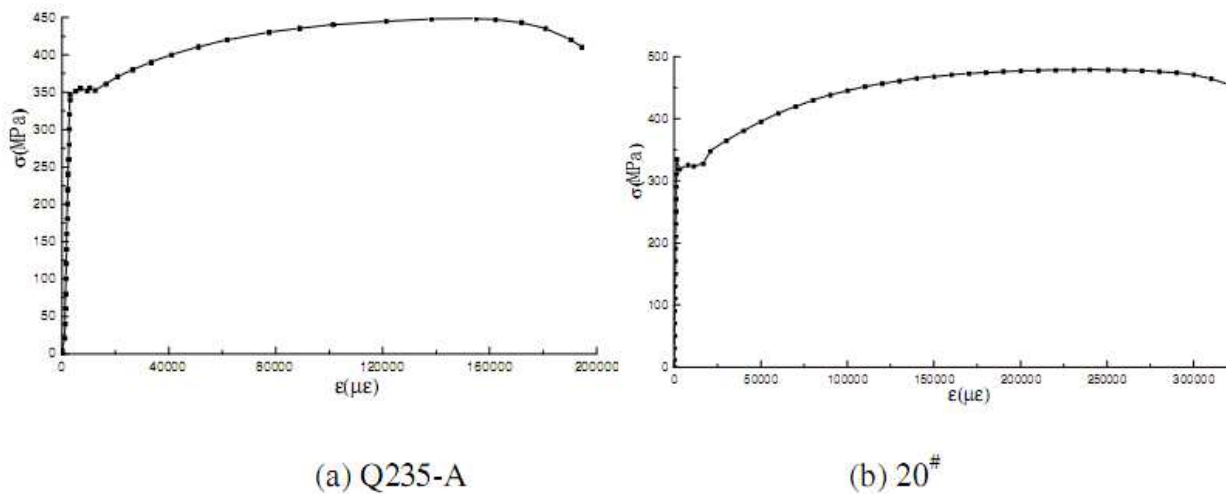

(a) Q235-A   (b) 20#

Figure 2. The curve of engineering stress-strain

2.2. Experimental setup

The local strains and nozzle displacements under in-plane moment on nozzle were measured to obtain the elastic stresses and deformation characteristics of the model vessels.The in-plane moment is applied as a force at the end of the nozzle, and the moment arm is the distance to the surface of the vessel.

Strain values at the typical measurement points of the cylinders and nozzles were measured using two element strain rosettes. Strain gages were mounted in the axial direction on the outside and inside surfaces for the cylinders, and on the outside surface only for the nozzles. Figure 3 illustrates the detailed locations of the strain gages for test vessel No. L_2.

Displacement values under in-plane moment (longitudinal loading direction) for the selected measurement points on the nozzle were measured using mechanical displacement sensors to obtain the load-displacement relationship in the elastic and plastic stages of the nozzles. A total of three displacement sensors were installed at locations along the nozzle length direction. The locations of the displacement sensors are indicated in Figure1.

Figure 4 is a photograph of test vessel No. L_1 during the test. The figure shows an obvious longitudinal deformation of the nozzle under the in-plane moment on the nozzle.
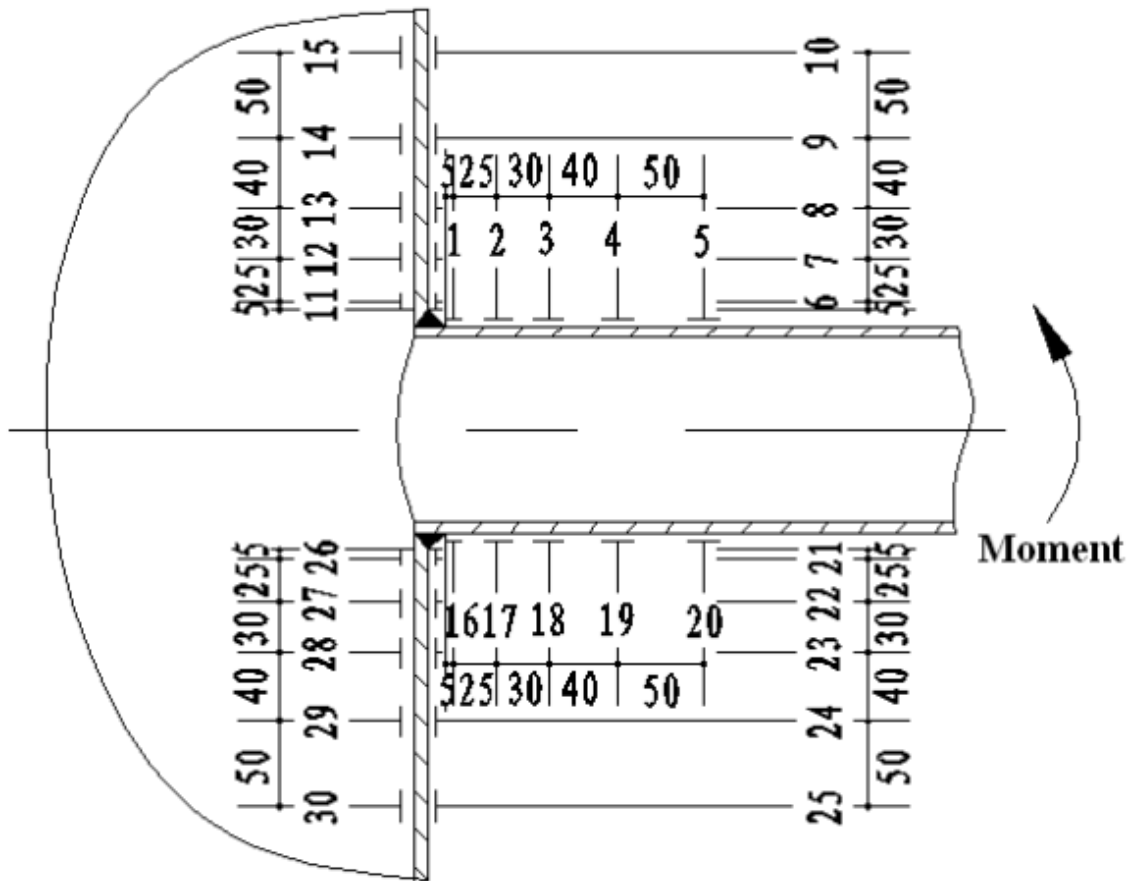
Figure 3. Locations of steain gages for model No. L2

Figure 4. Photo of model No L1 during the test

2.3. Experimental results

2.3.1. Plastic deformation behavior

Figure 5 indicates the elastic-plastic load deformation response at the three measurement points on the nozzle for model vessel No. L_2.
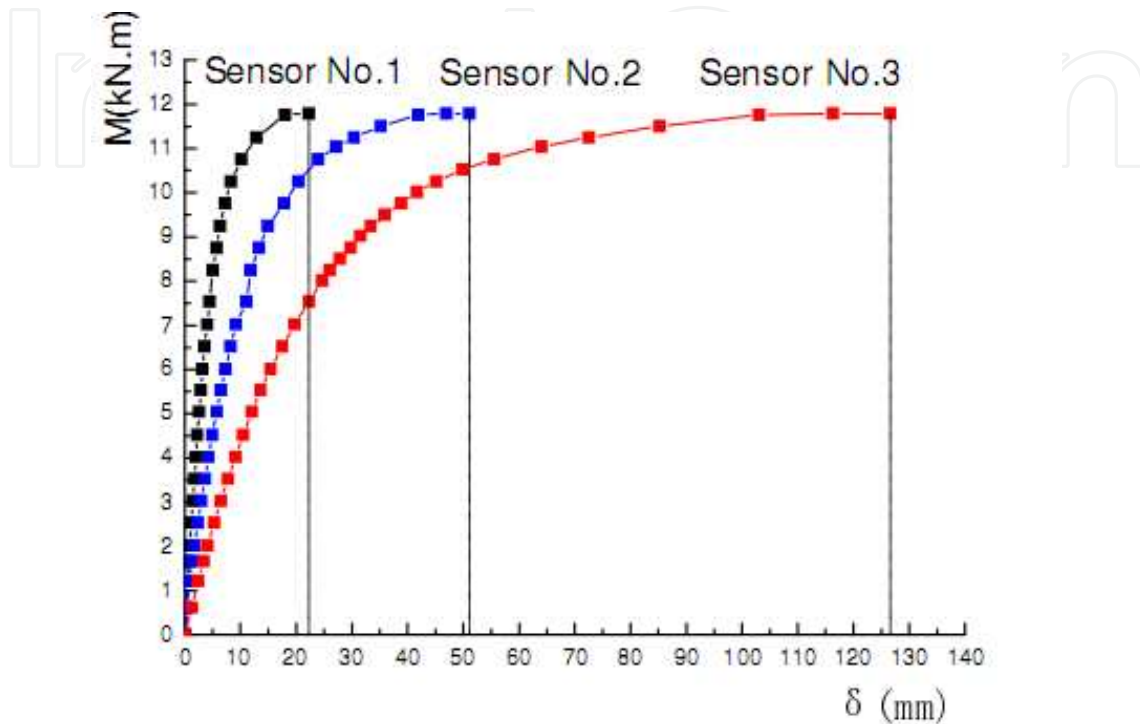

**Figure 5.** Load and elastic-plastic deformation response of nozzle

The intersection area of the nozzle and cylinder also produced an evident plastic deformation: the root of the nozzle moved into the vessel wall in the radial direction; as the cylinder yielded on the compression side of the cylinder and nozzle. Figure 6 shows an actual deformation state for test vessels No.$L_1$and No.L_2 under in-plane moment of 4.2kN.m and 7.5kN.m.

2.3.2. Plastic limit moment

Experimental plastic limit moments were obtained by the use of load versus displacement plots of the measurement points on the nozzle and load against strain curves of the key gauges located near the junction of the cylinder and nozzle. The plastic limit load is defined by applying the twice elastic slope criterion provided by the ASME Boiler and Pressure Vessel Code[1].

Figure 7 illustrates some typical load-displacement curves and corresponding limit moment for the sensor No.3.
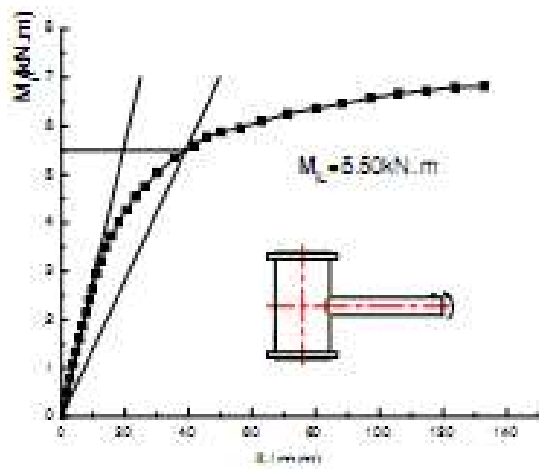
Figure 8 shows some typical load-strain curves and relevant limit moment of the strain gage No.6 as an example for the experiment vessels.
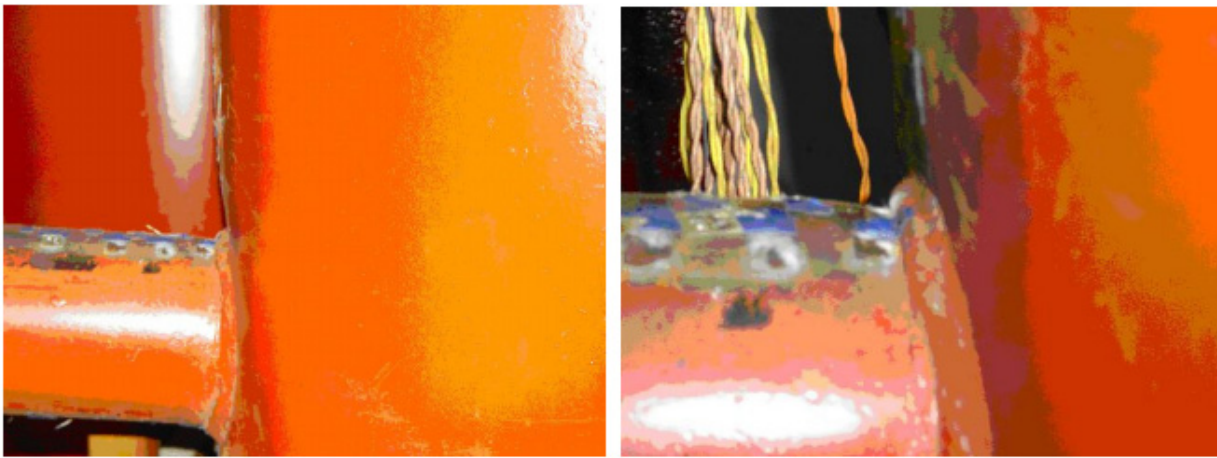
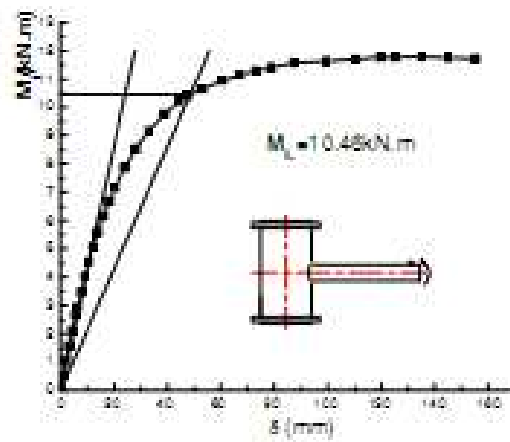(a) vessel No.L$_1$ (b) vessel No.L$_2$
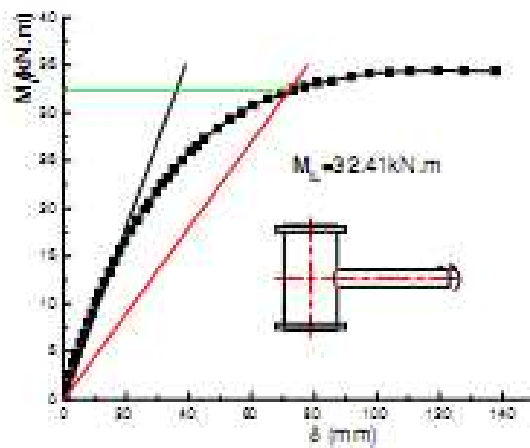
Figure 6. Load-deformation of the test vessels

(a) Load-displacement curves for L$_1$ vessel   (b) Load-displacement curves for L$_2$ vessel

(c) Load-displacement curves for L$_3$ vessel

Figure 7. Load-displacement curves for test models (Sensor No.3)
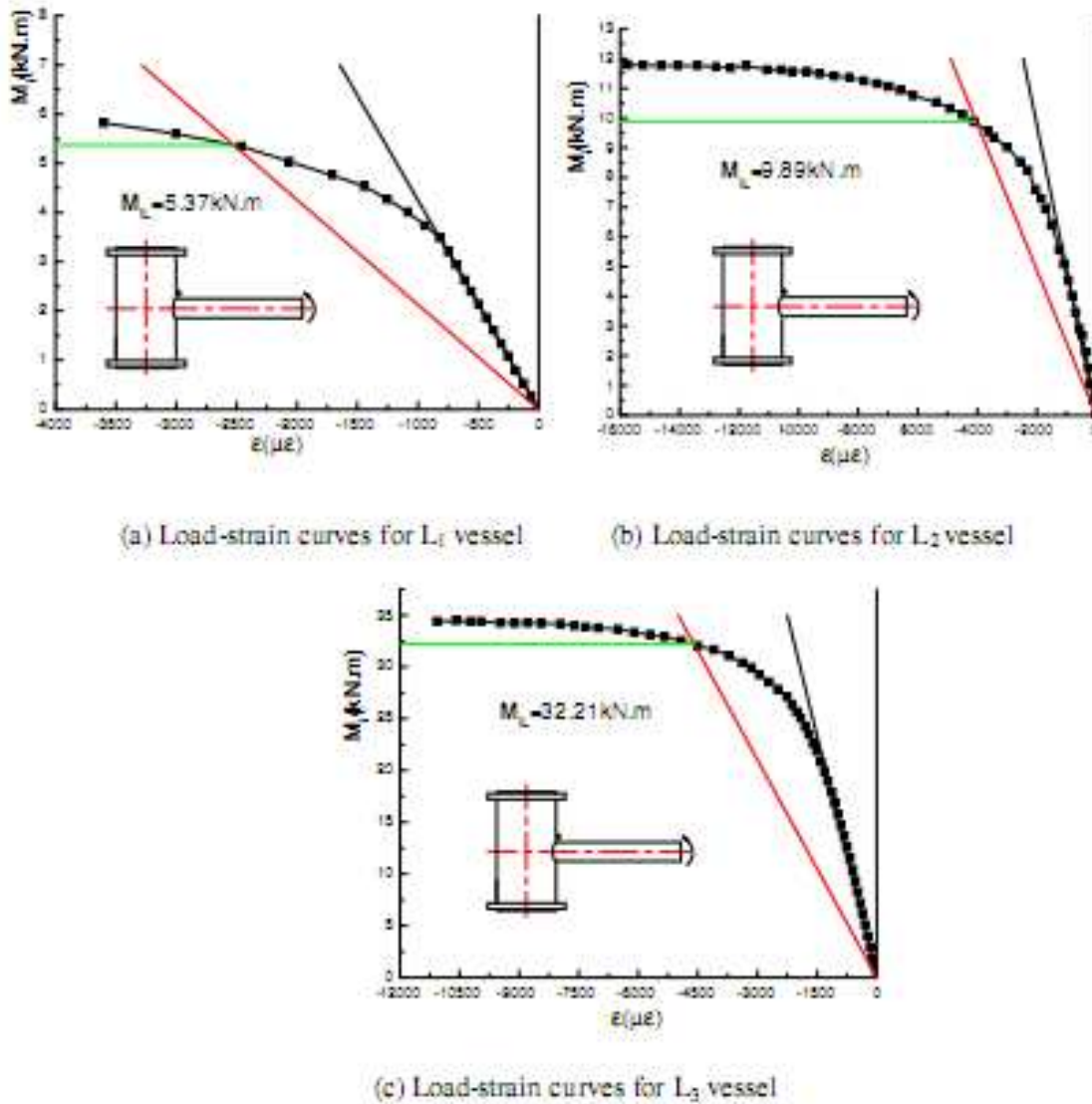
Figure 8. Load-strains curves for test models (Strains gage No.6)

Table 2 is a summary and comparison of the experimental plastic limit moment for the three model vessels. From the table, it is seen that the limit moments obtained by two measurement methods (displacement measuring and strain measuring) are in agreement. The maximum difference between the limit moments obtained from the two methods is 9.76%. For the same model vessel, the limit moments obtained using different measuring points also are in good agreement regardless of whether the measuring method is displacement measuring or strain measuring.

Models		L_1	L_2	L_3
By load-displacement method	Sensor No.1	5.96	10.81	33.42
	Sensor No.2	5.77	10.53	33.22
	Sensor No.3	5.50	10.46	32.41
	Average value	5.74	10.60	33.02
By load-strain method	Strain gage No.1	5.05	9.73	33.22
	Strain gage No.6	5.37	9.89	32.21
	Strain gage No.11	5.15	10.33	31.09
	Strain gage No.16	5.16	9.77	32.86
	Average value	5.18	9.93	32.35
Difference of the average value (%)		9.76	6.32	2.03

Table 2. Experimental results of plastic limit moment (kN.m)

3. Finite element analysis

3.1. Models and mesh

A static nonlinear finite element analysis of the experimental model vessels was carried out using the ANSYS code [15].Three-dimensional isoperimetric solid elements defined by eight nodes were used to generate the FEA mesh of the cylinder, nozzle and weld seam between the cylinder and nozzle. Two elements were used across the thickness of the shell.Due to the symmetry of the structure and loading, only one-half of the test vessel was modeled. Figure 9 illustrates the finite element mesh of the model vessel No.L_2.
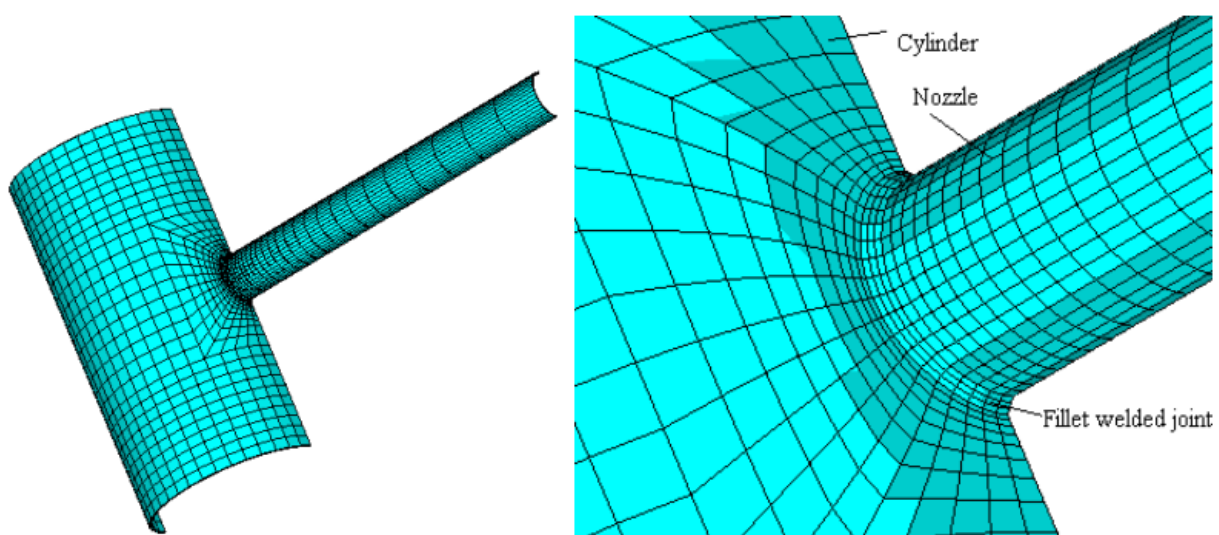

Figure 9. Finite element mesh for model vessel No.L_2

3.2. Boundary and loading conditions

The boundary conditions for the numerical simulation are the same as those used in the experimental portion of this study. One end of the cylinder is fixed, while the other end is free. All nodes on the symmetry section (longitudinal plane of the vessel) are constrained against displacement in the direction perpendicular to the symmetry plane. The FEA models were loaded a force at the end of the nozzle along the longitudinal direction of the vessels like in the experiment. For the purpose of comparing the results of the element analysis with those of the experiments, the same materials and loading increments as those of the test vessels were used. As a nonliner geometry analysis, the multilinear isotropic type of hardening behavior is used.A multi-linear elastic-plastic material model defined by nine points, as given in Table 3, was employed.

Material	Point	1	2	3	4	5	6	7	8	9
Q235-A	Stress (MPa)	355	357	378	403	432	463	485	510	519
	Strain ($\mu\varepsilon$)	1830	12232	20620	32698	49778	74576	96572	129445	158602
$20^{\#}$	Stress (MPa)	319	334	376	415	464	512	553	584	612
	Strain ($\mu\varepsilon$)	1477	16600	29567	48896	77066	113430	157103	198948	262455

Table 3. Material model

3.3. Analysis results

3.3.1. Plastic deformation

For the same loading condition as the experiment, the nozzle produced an obvious bending deformation and a depression of the cylinder on the compression side (in the longitudinal section) occurs. Figure 10 shows the local deformation characteristics which are consistent with those of the experiment (see Figure 4) for model vessel No. L2.

3.3.2. Plastic limit moment

Figure 11 indicates the load-displacement plots of simulation vessels from the sensor No.3 and corresponding limit moments on the nozzles.

At the same location as that of the experiment, load strain curves were plated in Figure 12, and corresponding limit moments for simulation vessels of strain gage No.6 were also shown in Figure 12.
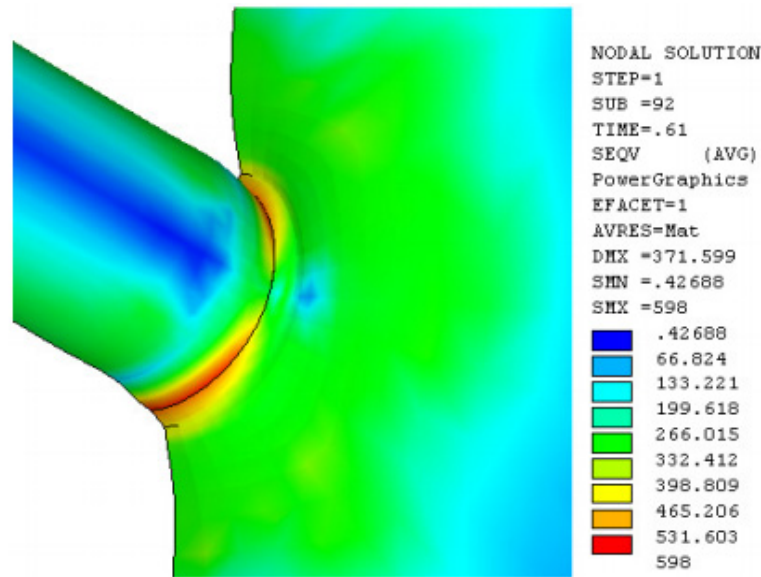
Figure 10. Local deformation for model NO. L$_2$ (M$_i$=13.05 kN.m)

(a) Load-displacement plots for L$_1$ vessel   (b) Load-displacement plots for L$_2$ vessel

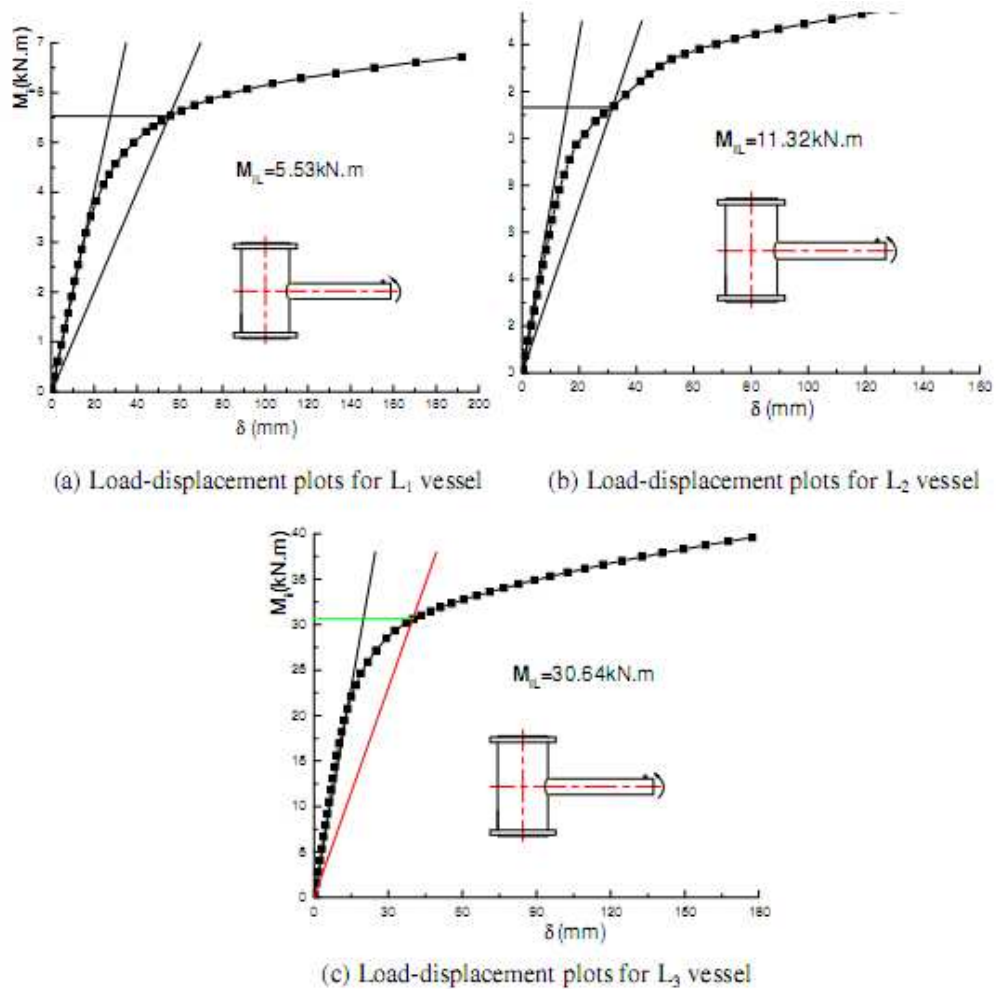(c) Load-displacement plots for L$_3$ vessel

Figure 11. Load-displacement plots for simulation models (Sensor No. 3)

The plastic limit moments for the three model vessels by FEA are listed in Table 4.

(a) Load-strain plots for L₁ vessel   (b) Load-strain plots for L₂ vessel

(c) Load-strain plots for L₃ vessel
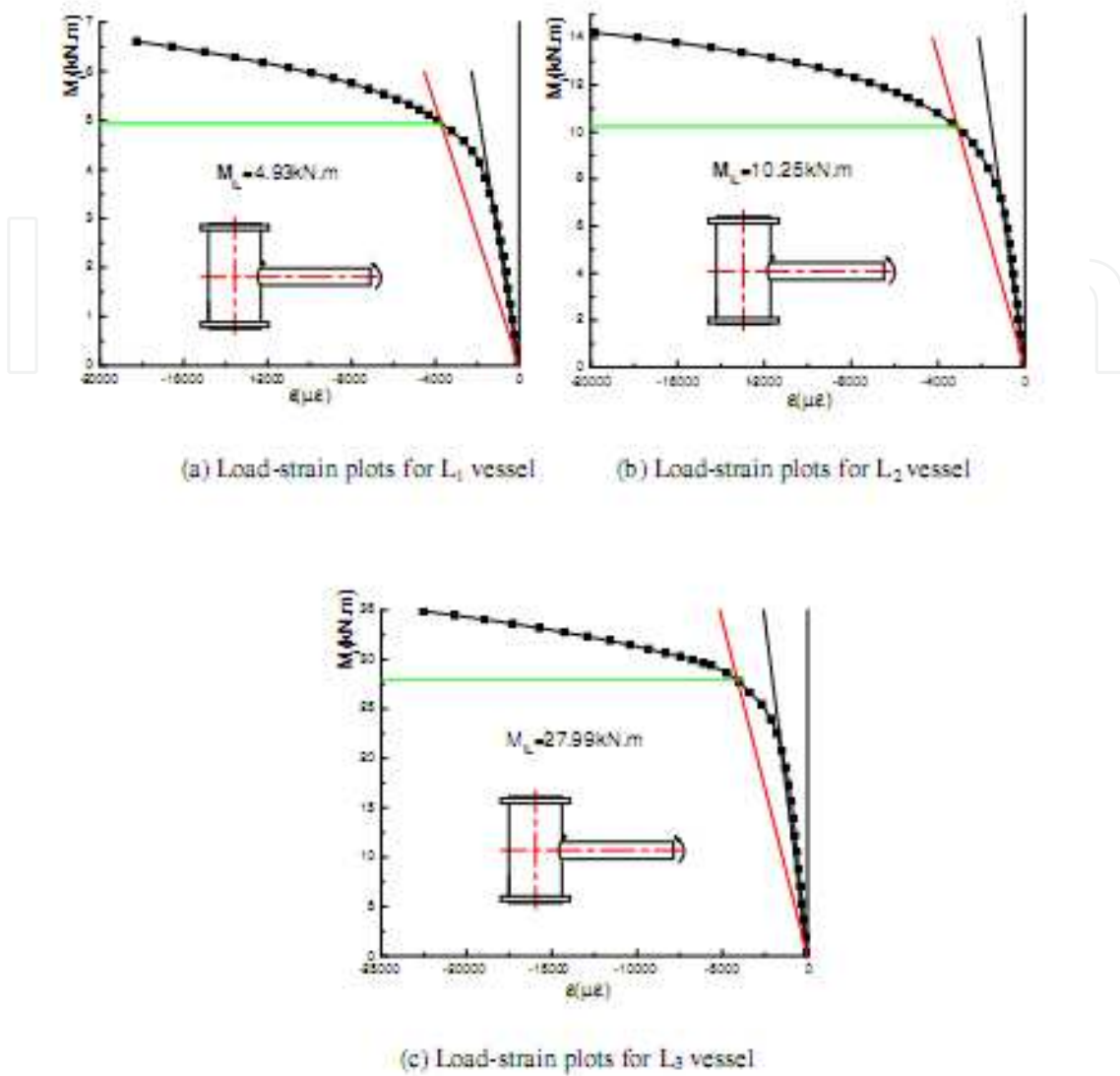
Figure 12. Load-strain plots for simulation models (Strain gage No. 6)

Models		L_1	L_2	L_3
By load-displacement method	Sensor No.1	5.27	11.67	30.38
	Sensor No.2	5.39	11.49	30.52
	Sensor No.3	5.53	11.32	30.64
	Average value	5.40	11.49	30.51
By load-strain method	Strain gage No.1	4.95	10.37	28.62
	Strain gage No.6	4.93	10.25	27.99
	Strain gage No.11	4.81	10.46	28.11
	Strain gage No.16	5.02	10.36	28.94
	Average value	4.93	10.36	28.42
Difference of the average value (%)		8.70	9.83	6.85

Table 4. FEA Results for the Plastic Limit Moment (kN.m)

4. Summary and comparison

From Tables 2 and 4, it is seen that the plastic limit moments from the displacement measurements are consistent with those determined from the strain measurements, whether by experimental method or finite element analysis.

Using an average of the values from different measuring points and displacement sensors, a summary and comparison of the twice-elastic-slope plastic limit load by experiment and finite element analysis for the three model vessels are shown in Table 5.

Model No.	D /T	d/ D	t/T	Limit-moment by Experiment (kN.m)			Limit-moment by FEA (kN.m)			Diffe-rence of the average value) (%)
				load-displacement method	load-strain method	avera-ge	load-displacement method	load-strain method	avera-ge	
L₁	62.5	0.172	0.375	5.74	5.18	5.46	5.40	4.93	5.17	5.31
L₂	62.5	0.246	0.50	10.60	9.93	10.27	11.49	10.36	10.93	6.43
L₃	62.5	0.428	0.625	33.02	32.35	32.69	30.51	28.42	29.47	9.85

Table 5. Summary and comparison of plastic limit moment

From Table 5, it can be seen that the results for the plastic limit moment from experiment and finite element analysis including displacement and strain measuring techniques are in good agreement. The difference between experiment and finite element analysis is within 10%.

5. Parametric analysis and correlation equation

5.1. Parametric finite element modeling

On the basis of the previous studies, parametric modeling was performed. The sets of parameters of the analysis models used in this part of the study are given in Table 6. A total of 64 configurations were analyzed to investigate the relationship between the various geometric parameters and plastic limit moments of the vessel-nozzle structures. The data in Table 7 were obtained from the finite element analysis of 64 models.

5.2. Correlation equation

A correlation equation for plastic limit load of cylindrical vessels under in-plane moment on the nozzle can be obtained by using the data from Table 7 and the software package Statistica (non-linear regression). The resulting correlation equation for the plastic limit moment on the nozzle is as follows:

$$M_{iL} = [-0.0148 + 0.704\left(\frac{d}{D}\right) + 1.845\left(\frac{d}{D}\right)^2]\left(\frac{d}{D}\right)^{-1.761}\left(\frac{t}{T}\right)^{-0.555}\left(\frac{D}{T}\right)^{-0.476} M_b$$

Where, M_b is the limit load of a straight nozzle,

$$M_b = d^2 t \, \sigma_s \, [8] \, (kN.m)$$

This equation holds for the following range of parameters:

$$0.1 \leq d/D \leq 0.4 \, , \, 0.25 \leq t/T \leq 1 \, , \, 50 \leq D/T \leq 125 \, , \, 500mm \leq D \leq 2000mm$$

Model	d/D	t/T	D/T
1	0.1	0.25	50
2	0.1	0.5	75
3	0.1	0.75	100
4	0.1	1.0	125
5	0.2	0.25	75
6	0.2	0.5	50
7	0.2	0.75	125
8	0.2	1.0	100
9	0.3	0.25	100
10	0.3	0.5	125
11	0.3	0.75	50
12	0.3	1.0	75
13	0.4	0.25	125
14	0.4	0.5	100
15	0.4	0.75	75
16	0.4	1.0	50

Table 6. Primary parameters of the FE models

Models	Limit Moment			
	D=500mm	D=1000mm	D=1500mm	D=2000mm
1	2.25	16.43	64.37	156.52
2	3.11	22.56	88.98	216.47
3	3.52	25.58	97.96	231.89
4	3.12	24.27	79.05	185.34
5	5.63	43.73	161.53	398.26
6	18.31	142.05	539.24	1307.58
7	6.51	50.14	158.86	367.96
8	11.52	85.09	282.45	632.46
9	9.47	73.76	275.15	608.14
10	11.67	83.05	276.31	650.87
11	58.02	434.86	1536.42	3500.24
12	36.21	256.45	853.13	2068.57
13	13.37	109.21	363.01	548.12
14	27.52	204.18	680.76	1358.54
15	52.54	360.04	1221.85	2808.47
16	118.34	836.42	2804.57	6618.21

Table 7. Limit loads of the FE models (kN.m)

In order to verify the accuracy of the correlation equation, the plastic limit moments of three models were calculated and compared with those from the experimental and FEA studies as seen in Table 8.

Models	L_1	L_2	L_3	Models	L_1	L_2	L_3
Limit-moment by Regression Equation (M_{EQU})	5.55	11.53	33.63	Limit-moment by Regression Equation (M_{EQU})	5.55	11.53	33.63
Limit-moment by Experiment (M_{EXP})	5.46	10.27	32.69	Limit-moment by FEA (M_{FEA})	5.17	10.93	29.47
Difference ($\dfrac{\left\| M_{EQU} - M_{EXP} \right\|}{M_{EQU}}$)	1.62%	10.93%	2.80%	Difference ($\dfrac{\left\| M_{EQU} - M_{FEA} \right\|}{M_{EQU}}$)	6.85%	5.20%	12.57%

Table 8. Comparison of plastic limit moment (kN.m)

6. Conclusions

Experiments and comparative 3D-nonlinear finite element analyses of cylindrical vessel-nozzle connections subjected to an in-plane moment on the nozzle were carried out. In addition, an extensive geometric parameter study of such joints was performed with FEA.The following general conclusions can be drawn from these studies:

1. The experimental and 3D-nonlinear finite element analyses including load-strain and load-displacement of the nozzle responses provide effective and reliable determination methods for the pressure vessel-nozzle (or main-branch pipe) connections subjected to external loads on the nozzle.
2. The plastic limit moments determined from experimental and finite element analysis studies are in good agreement. The maximum error of the average experimental versus FE calculated limit moments is about 10%.
3. The limit moments from load-displacement and load-strain curves are in reasonable agreement for the analyzed geometry.
4. The plastic limit moments from experimental and finite element analysis studies are greatly increased with an increase of d/D, t/T ratios of the model vessels.
5. The correlation equation provided in this paper can be used to determine, within reasonable limits, the plastic limit moment of cylinder-nozzle connections subjected to an in-plane load on the nozzle.

Author details

B.H. Wu

Department of Mechanical and Power Engineering, Nanjing University of Technology, Nanjing, People's Republic of China

7. References

[1] ASME Boiler and Pressure Vessel Code, 2004 edition, section Ⅷ, Division 2, American Society of Mechanical Engineering, New York.

[2] Ellyin, F., 1976, "Experimental Investigation of Limit Loads of Nozzles in Cylindrical Vessels,"Welding Research Council Bulletin, No.219, WRC, New York.

[3] Ellyin, F., 1977, "An Experimental Study of Elastic-plastic Response of Branch Pipe Tee Connection Subjected to Internal Pressure, External Couples and Combined Loadings," Welding Research Council Bulletin, No.230, WRC, New York.

[4] Schroeder, J., 1985, "Experimental Limit Couples for Branch Moment Loads on 4-in. ANSI B16.9 Tees,"Welding Research Council Bulletin, No.304, WRC, New York.

[5] Junker, A.T., 1985, "Finite Element Determination of the Limit Load of a Nozzle in a Cylindrical Vessel Due to In-plane and Out-of-plane Moments," Swanson Engineering Associates Corporation (SEAC) Report No.SEAC-TR-312,Rev.2, to the Pressure Vessel Research Committee, WRC, New York.

[6] Moffat, D.G., 1985, "Experimental Stress Analysis of Four Fabricated Equal Diameter Branch Pipe Intersections Subjected to Moment Loadings and Implications on Branch Junction Design," Proc Instn. Mech. Engrs., Vol.199, No.4, PP. 261~284.

[7] Moffat, D.G., 1991, Mwenifumbo, J.A.M., Xu, S. H. and Mistry, T., "Effective Stress Factors for Piping Branch Junctions Due to Internal Pressure and External Moment Loads," Journal of Strain Analysis, Vol.26, No.2, PP.85~101.

[8] Rodabaugh, E.C., 1988, "A Review of Area Replacement Rules for Pipe Connections in Pressure Vessels and Piping,"Welding Research Council Bulletin, No.335, WRC, New York.

[9] Rodabaugh, E.C., Interpretive report on limit analysis and plastic behavior of piping products, Welding Research Council Bullition No.254,1976

[10] Kalnins, A., 2001, "Guidelines for Sizing of Vessels by Limit Analysis,"Welding Research Council Bulletin, No.464, WRC, New York.

[11] Chapuliot, S., Moulin, D., and Plancg, D., 2002, "Mechanical Behavior of a Branch Pipe Subjected to Out-of-plane Bending Load," ASME Journal of Pressure Vessel Technology, Vol.124, PP.1~14.

[12] Mourad Hashem, M., Maher, Y.A., 2002, "Limit-Load analysis of Pipe Bend under Out-of-plane Moment and Internal Pressure," ASME Journal of Pressure Vessel Technology, Vol.124, PP.7~32.

[13] Widera, G.E.O., Wei, Z., 1998, "Parametric Finite Element of Large Diameter Shell Intersection," Part 2, External Loading, PVRC Project No.96-20AS, WRC, New York.

[14] Sang, Z.F., Wang, Z.L., Xue, L.P., Widera, G..E.O., 2005, "Plastic Limit Loads of Nozzles in Cylindrical Vessels under Out-of-plane Moment Loading," International Journal of Pressure Vessels and Piping, 82, PP. 638-648.

[15] Swanson Analysis System Inc., "ANSYS Engineering Analysis Systems User's Manual".